Electronic Supplementary Information

Target-triggered dynamic hairpin assembly for signal amplification of microRNA and oncogene and its application in live-cell imaging

Yuanfang Li,[‡a] Shuzhen Yue,[‡a] Hongjie Qi,[a] Caifeng Ding,[b] Weiling Song[b] and Sai Bi*[a]

[a]University-Industry Joint Center for Ocean Observation and Broadband Communication, College of Chemistry and Chemical Engineering, Qingdao University, Qingdao 266071, P. R. China.

[b]Laboratory of Optic-electric Sensing and Analytical Chemistry for Life Science，MOE; Shandong Key Laboratory of Biochemical Analysis; Key Laboratory of Analytical Chemistry for Life Science in Universities of Shandong; College of Chemistry and Molecular Engineering, Qingdao University of Science and Technology, Qingdao 266042, P. R. China

*Corresponding author. E-mail: bisai11@126.com.

‡These authors contributed equally to this work.

Experimental Section

Materials and Reagents. All oligonucleotides used in this study were synthesized and purified by Sangon Biotech Co., Ltd. (Shanghai, China). Their sequences are listed in Table S1 and the secondary structures of hairpins are shown in Figure S1. The oligonucleotides were prepared to a final concentration of 100 μM and stored in DNase/RNase-free ultrapure water at -20 °C. Tris (hydroxymethyl) aminomethane (Tris), ethylenediaminetetraacetic acid disodium salt (EDTA-2Na) and magnesium chloride ($MgCl_2$) were ordered from Aladdin Chemistry Co., Ltd. (Shanghai, China) In all experiments, the TE buffer (10 mM Tris-HCl, 1 mM EDTA-2Na, pH 7.4) containing 12.5 mM $MgCl_2$ was used to dilute the DNAs and miRNAs. MCF-7 cells, HeLa cells, L-02 cells and MDA-MB-231 cells were all purchased from Sixin Biotechnology Co., Ltd. (Shanghai, China). All the reagents were of analytical grade and used without further purification. DNase/RNase-free ultrapure water was used in all experiments.

Table S1. Oligonucleotides sequences used in this work[a]

name	Sequence 5'-3'
I (miR-21)	UAGCUUAUCAGACUGAUGUUGA
H_a	Dabcyl-TCAACATCAGTCTGATAAGCTATACACGATCTAGCTGTTGATTATCAGACTGA-FAM
H_b	TCAGTCTGATAATCAACAGCTATACACGATCTAGCGACTGATGTTGATTATCA
H_c	TGATAATCAACATCAGTCGCTATACACGATCTAGCTTATCAGACTGATGTTGA
sm miR-21	UATCUUAUCAGACUGAUGUUGA
tm miR-21	UATCUAAUUAGACUGAUGUUGA
miR-155	UUAAUGCUAAUCGUGAUAGGGGU
H_a'	Dabcyl-TCAACATTAGTCTGATAAGCTATACACGATCTAGCTGTTGATTATCAGACTAA-FAM
H_b'	TTAGTCTGATAATCAACAGCTATACACGATCTAGCGACTAATGTTGATTATCA
H_c'	TGATAATCAACATTAGTCGCTATACACGATCTAGCTTATCAGACTAATGTTGA
H_d	Dabcyl-TCAACATCAGTCTGATAAGCTACTTCCAATCACAACAGTAGCTT ATCAGACTGA-FAM
H_e	TGATAAGCTACTGTTGTGATTGGAGACTGATGTTGATCCAATCACAACAGTAGC
H_f	GTTGTGATTGGATCAACATCAGTCAGTAGCTTATCAGACTGATGTTGATCCAAT
I_0 (BRCA1 oncogene)	GTGTTTTTCATAAACCCATTATCCAGGACTGTTTATAGCTGTTGGAAG
H_u	Dabcyl-CTTCCAACAGCTATAAACAGTCCTTACACGTACAGGACTTGGAAGGTTTATAGCTGT-FAM
H_v	ACAGCTATAAACCTTCCAAGTCCTCCTCGCAATAGGACTAGCTGTTGGAAGGTTTAT
H_w	ATAAACCTTCCAACAGCTAGTCCTTGATTGGAGAGGACTGTTTATAGCTGTTGGAAG
H_x	Dabcyl-TTCATAAACCCAGTGTTTTTATCCGTACGTGTAGGATAATGGGTTTATGAAAAACAC-FAM
H_y	AACCCAGTGTTTTTCATATTATCCATTGCGAGGGGATAAAAACACTGGGTTTATGAA
H_z	GTGTTTTTCATAAACCCATTATCCCTCCAATCAGGATAATATGAAAAACACTGGGTT

[a] The mismatched bases are underlined.

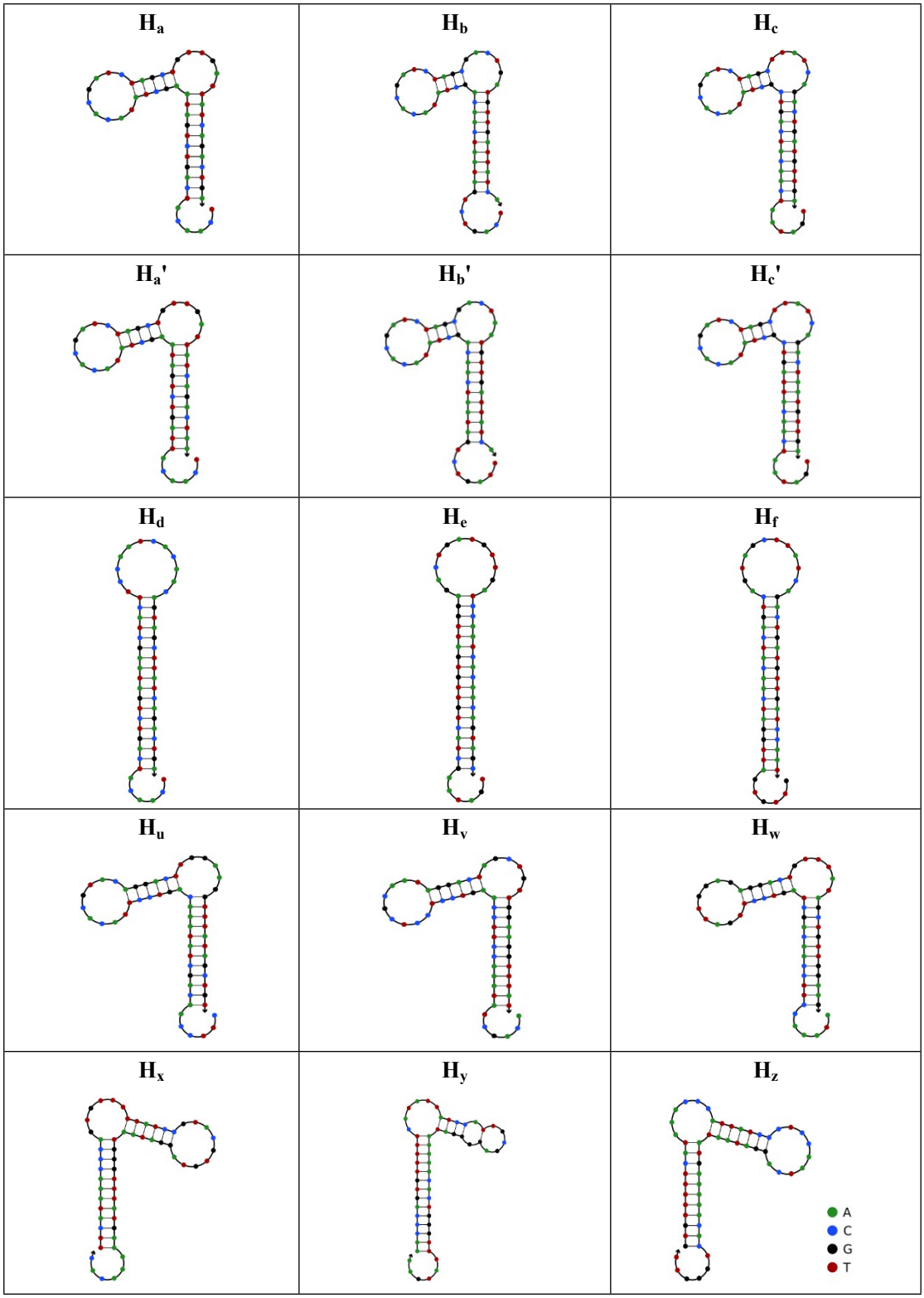

Fig. S1 Secondary structures of hairpin species used in this study, which are predicted using the NUPACK software (www.nupack.org).

Preparation of DNA Hairpins. Before experiments, all the DNA hairpins were respectively prepared in TE buffer and annealed on a thermal cycler by heating at 95 °C for 5 min, gradually cooling to 25 °C at a rate of 0.1 °C/s, and standing at 25 °C for 3 h at least to obtain the desirable and stable secondary structures.

Native Polyacrylamide Gel Electrophoresis (PAGE). Firstly, 15% non-denaturing PAGE was prepared by mixing 4 mL of 30% acrylamide/bis-acrylamide gel solution, 3756 μL of deionized water, 160 μL of 50× TAE buffer (pH 8.0), 80 μL of 10% ammonium persulfate (APS) and 4 μL of N,N,N,N'-tetramethylethylenediamine (TEMED). After polymerization for 40 min, the resulting gel was soaked in 1× TAE buffer (pH 8.0). Then, 12 μL of the sample was first mixed with 2 μL of 10× loading buffer, and then the samples were added into the gel, respectively. At room temperature, electrophoresis was run at 170 V for 5 min and 110 V for 80 min. After staining in diluted 4S Red Plus solution (Sangon Biotech. Co., Ltd., China) for 30 min, the gel was photographed by a Tanon 2500R UV gel imaging system (Tanon Science & Technology Co., Ltd., China).

Atomic Force Microscopy (AFM) Imaging. The DNA products were directly visualized by AFM imaging. The samples were prepared as follows. A 3 μL of each annealed hairpin (2 μM for each) was mixed with 3 μL of initiator (miR-21 or BRCA1 oncogene, 1 μM) or 3 μL of TE buffer, followed by reaction at 25 °C for 6 h. Before imaging, the resulting products were washed with 30 μL of deionized ultrapure water three times by centrifugation at 10 000 rpm for 3 min. Then, 10 μL of each sample was deposited onto the surface of freshly cleaved mica and left to dry under ambience air. AFM imaging experiments were performed in air under the tapping mode using Being Nano-Instruments CSPM-4000 system (Benyuan, China), and the results were analyzed with CSPM Console software (Benyuan-CSPM4000, China).

Real-Time Fluorescence Monitoring. The real-time fluorescence was monitored to verify the kinetics of the dynamic self-assembly process initiated by different concentrations of target miR-21 or BRCA1 oncogene. Briefly, 2 μL of each annealed hairpin (10^{-5} M for each, pH 7.4) were mixed with 2 μL of miR-21 or BRCA1 oncogene with different concentrations. Upon the supplemental TE buffer was added into the mixture to a final volume of 40 μL, the sample was immediately monitored on a LineGene 4800 Real-Time fluorescence detector (Hangzhou, China) with an interval of 30 s for 6 h totally (λ_{ex} = 480 nm and λ_{em} = 520 nm). The reaction temperature was set as 25 °C.

Cell Culture and Transfection. The transfection reagent (1 mL total volume) was the mixture of

two different solutions. The first solution was the mixture (500 μL) of detection probes (A, B and C) with Opti-MEM and the other was the mixture (500 μL) of Lipohigh transfection reagent (4 μL) with Opti-MEM, which was finally kept standing for 25 min after adequately mixing. Cells were first cultured in DMEM media supplemented with 10% fetal bovine serum, 100 mg/mL penicillin and 100 mg/mL streptomycin at 37 ^{o}C for 16 h in a humidified atmosphere containing 5% CO_2 and 95% air. The cells were plated on the sterilized glass bottom in 30 mm confocal dish at a density of 10^5 cells. After washing the cells with PBS, the cells were incubated at 37 ^{o}C for 4 h with 1 mL of prepared Lipohigh transfection liquid solution which contained probes (200 nM for each) under the condition with 5% CO_2.

Confocal laser scanning microscopy (CLSM) imaging. Before imaging, the transfection reagent was removed from the confocal dishes. After washing with PBS buffer (pH 7.4, 0.01 M) three times, the cultured cells were added into the fresh PBS culture medium in the confocal dishes. Ultimately, the fluorescent images were recorded on a Leica TCS SP8 inverted confocal microscope (Leica, Germany) in the green channel with the excitation at 488 nm and emission at 510-540 nm.

Flow Cytometry Analysis. The MCF-7 cells were seeded on a six-well culture plate at 10^5 cells/well and the culture procedure was the same as that mentioned above. After washing three times with PBS, MCF-7 cells were trypsinized to detach from the culture plate. Then, the suspended cell solution was centrifuged at 1 000 rpm for 3 min and the cells were washed with PBS three times. Finally, MCF-7 cells were resuspended in PBS and subjected to flow cytometric detection under 488 nm excitation. The fluorescence intensities represented 10 000 analyzed cells.

Cytotoxicity Evaluation. After transfection with hairpin probes for 4 h as mentioned above, the cell viabilities were measured by the Cell Counting Kit-8 (CCK-8) assay. In brief, MCF-7 cells, HeLa cells, L-02 cells and MDA-MB-231 cells seeded in 96-well plate (1.5×10^4 per well) were added 10 μL of CCK-8 solution and incubated for 2 h at 37 ˚C. Finally, the microplate reader was used to detect the absorbance of cancer cells at 450 nm. The cell viability was determined by (Mean $Absorb_{test}$ - Mean $Absorb_{blank}$/ Mean $Absorb_{control}$ - Mean $Absorb_{blank}$)×100%.

Quantitative Detection of Intracellular MiRNA-21. HeLa cells were incubated in confocal dish at 10^5 cells/mL, and were firstly transfected miRNA-21 mimics with increasing amounts of 0, 0.4, 0.7, 1.1, 1.6 pg/cell for 1 h. The average amount of miRNA-21 mimics which were transfected into each cell was measured by UV absorbance at 260 nm. The cells were incubated at 37 ˚C for 4 h with

1 mL of prepared Lipohigh transfection liquid solution which contained the probes (200 nM for each) under the condition with 5% CO_2, and then were washed with PBS to record the confocal fluorescence images.

Additional Results and Discussion

Non-Denaturing PAGE Characterization of Unidirectional DHA. The reaction pathways of the unidirectional DHA were first characterized by non-denaturing PAGE. As shown in Fig. S2, when 1× I is mixed with H_a, a band that corresponds to $I{\cdot}H_a$ is produced (lane 1). After H_b is introduced, a new band can be observed that corresponds to $I{\cdot}H_a{\cdot}H_b$ (lane 2). Upon H_c is added into the $I{\cdot}H_a{\cdot}H_b$ with a ratio of 1:1, the hybrid of $I{\cdot}H_a{\cdot}H_b{\cdot}H_c$ is produced (lane 3). In particular, when 0.5× I react with 1× hairpins, the DNA nanostructures with big molecular weight are formed, which can be easily observed at a shorter electrophoresis distance (lane 4). Fortunately, in the absence of I, the hairpins can metastably coexist without leakage (lane 5). Therefore, the above gel shifting results validate the feasibility of the proposed DHA strategy step-by-step.

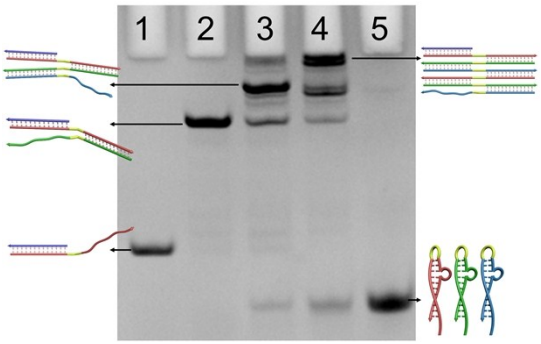

Fig. S2 Native PAGE of the reaction pathways of the DHA. lane 1: 1× I + H_a; lane 2: 1× I + H_a + H_b; lane 3: 1× I + H_a + H_b + H_c; lane 4: 0.5× I + H_a + H_b + H_c; lane 5: H_a + H_b + H_c. The concentration of each hairpin initially added is 2 μM (1×). The reactions are performed at 25 °C for 6 h.

Traditional CHA. The reaction pathways of traditional CHA were verified by native PAGE (Fig. S3B). When 1× I is mixed with H_d, a band that corresponds to $I{\cdot}H_d$ is produced (lane 1). After H_e is introduced to the resulting $I{\cdot}H_d$, a new band can be observed that corresponds to $I{\cdot}H_d{\cdot}H_e$ (lane 2). When 1× I (lane 3) and 0.5× I (lane 4) respectively react with the mixture of H_d, H_e and H_f, the three-arm DNA junctions are formed with the recycling of I to catalyze another CHA process. The band in lane 5 corresponds to the mixture of hairpins H_d, H_e and H_f in the absence of I, indicating

no leakage occurs without I. It should be noted that in comparison with lanes 3 and 4, even if the concentration of I decreases, no hybrid with larger molecular weight is generated, thus indicating that the product is always the three-arm DNA junction. This phenomenon can be attributed that in the traditional CHA no spacer is designed in the hairpin species, so the initiator strand can be easily displaced by H_f during CHA, resulting in the formation of three-arm DNA junction.

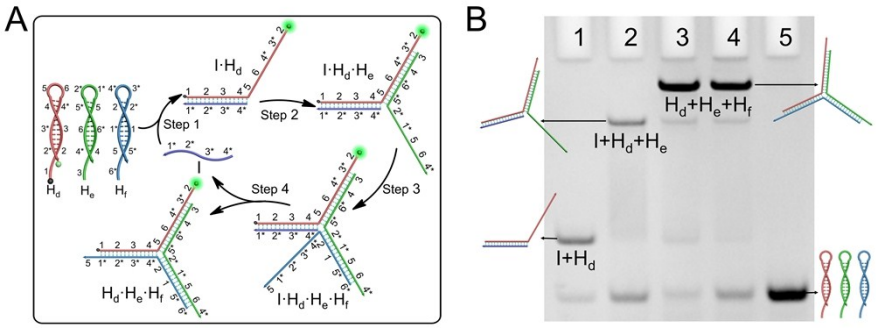

Fig. S3 Traditional CHA. (A) Schematic representation of CHA. (B) Native PAGE of the reaction pathways of CHA. lane 1: 1× I + H_d; lane 2: 1× I + H_d + H_e; lane 3: 1× I + H_d +H_e + H_f; lane 4: 0.5× I + H_d + H_e + H_f; lane 5: H_d + H_e + H_f. The concentration of each hairpin initially added is 2 μM (1×). The reactions are performed at 25 °C for 6 h.

DHA for In-Situ Imaging of Intracellular MiRNAs. After transfecting the hairpin probes for 4 h, the cell viabilities were confirmed by CCK-8 assay and the results are shown in Fig. S4.

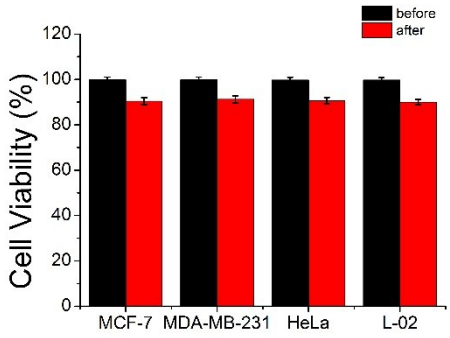

Fig. S4 Cell viability study by CCK-8 assay before (black) and after (red) transfection of the hairpin probes (MCF-7 cell, 90.43%; MDA-MB-231 cells, 91.20%; HeLa cells, 90.68%; L-02 cells, 90.03%).

The ability of the DHA to identify the expression level of miR-21 in MCF-7 cells was then studied (Fig. S5). Herein, MCF-7 cells were separated into three groups in parallel for miR-

21 imaging. Group one was the control sample which was treated with DHA. Group two was the miR-21 mimics transfected MCF-7 cells, which was used to increase the intracellular target amount. Group three was the miR-21 inhibitor sequence transfected MCF-7 cells to knock down the content of intracellular miR-21. The results show that the increased fluorescence signal can be easily observed when miR-21 mimics are transfected into MCF-7 cells, and nearly no fluorescence is seen after transfecting miR-21 inhibitor into cells since the inhibitors can knock down the content of miR-21 through hybridization events. These results evidently demonstrate that the DHA-based bioimaging strategy is closely related to the expression level of intracellular miR-21, which thus has the ability to analyze the changes of miRNAs in live cells.

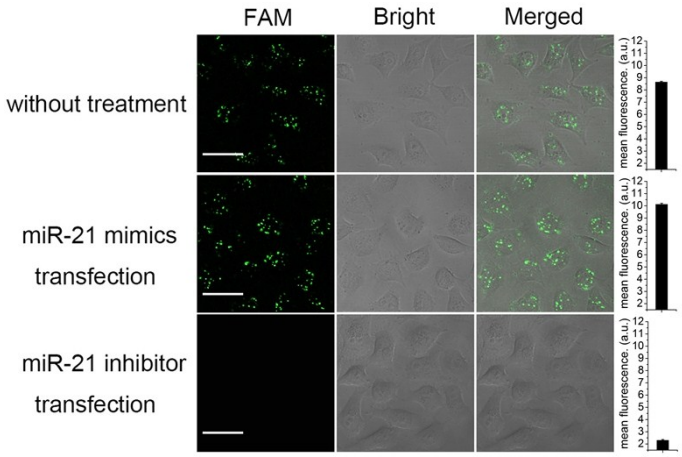

Fig. S5 CLSM imaging of miR-21 in MCF-7 cells without treatment or pretreated with miR-21 mimics (100 nM) and miR-21 inhibitor (100 nM) for 1 h at 37 °C, respectively. The concentration of each hairpin is 200 nM. Error bars indicate the standard deviations of three independent measurements. Scale bar: 20 μm.

Moreover, the quantitative detection of miR-21 in Hela cells has been studied. From Fig. S6, different concentrations of miR-21 mimics were transfected into Hela cells, and the corresponding CLSM images were recorded. The plot of fluorescence intensity versus the amounts of miRNA-21 mimics transfected into Hela cells showed a good linear relationship with a linear regression equation of $I = 2.79C_{\text{miR-21 mimic}} + 4.56$ and a related coefficient of 99.82%, and the average quantity of miRNA-21 in a single HeLa cell was calculated as 1.64 pg. Therefore, the proposed DHA strategy

can be readily applied to quantify the intracellular miRNA.

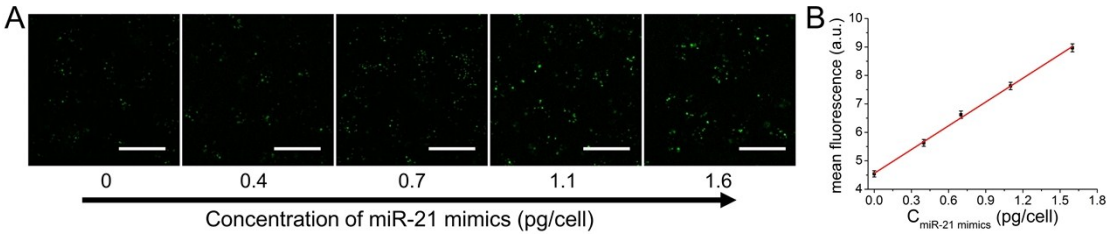

Fig. S6 (A) CLSM imaging of miR-21 in HeLa cells pretreated with different concentrations of miR-21 mimics for 1 h at 37 °C. Scale bar: 20 μm. (B) Corresponding plot of mean fluorescence intensity versus the amount of transfected miRNA-21 mimics derived from (A). Error bars indicate the standard deviations of three independent measurements. The concentration of each hairpin is 200 nM.

Bilateral Growth Mechanism. Besides one-side growth mechanism, our proposed DHA was further applied to a bilateral growth manner, which achieved sensitive and selective detection of DNA with long sequences (Fig. S7A). Briefly, the system consists of six hairpins (H_u, H_v, H_w, H_x, H_y and H_z) and an initiator (I_0, BRCA1 oncogene with 48 nt). Similar to the hairpin structures mentioned above, a spacer sequence shown as domain 's' is designed in each hairpin. In the absence of I_0, the dynamic assembly is kinetically hindered. Since the I_0 strand contains the recognition site at both 3' and 5' ends of H_u and H_x, respectively, upon I_0 is added, H_u and H_x are opened through toehold-mediated SDRs, leading to the release of two single-stranded regions of H_u and H_x. Then, according to the mechanism of DHA, hairpins H_v (or H_y), H_w (or H_z) are opened through toehold-mediated SDRs triggered by the newly exposed single-stranded domains and finally result in the formation of DNA nanobrush structures which grows in a bidirectional manner. The reaction mechanisms were confirmed by AFM (Fig. S7B). In comparison with the unidirectional hairpin assembly, the DNA nanobrushes grown in the bilateral DHA are generally longer since the hairpins can be assembled in both directions simultaneously.

The real-time fluorescence was further carried out to investigate the kinetics of the bilateral DHA by labeling quencher (Dabcyl) and fluorophore (FAM) at 5' and 3' ends of

both H_u and H_x (Fig. S7C). In the absence of I_0 (the blank), the fluorophore and the quencher are at a close proximity spatially and thus the fluorescence signal is low. Upon addition of I_0, the DHA reaction is activated bilaterally and the fluorescence of FAM is restored, which thus results in an intensified fluorescence intensity. The calibration curve is plotted with the fluorescence intensity at 6 h versus the final concentration of I_0. The fluorescence signals are enhanced with the increase of the concentration of I_0 from 0.005× to 1×. From the insert calibration curve depicted in Fig. S7D, the target DNA can be sensitively detected with a linear range from 2.5 to 25 nM (finally concentration) and a detection limit of 1.03 nM (3σ). In comparison with the detection limit obtained by the unidirectional DHA (1.88 nM), nearly 2-fold improved detection sensitivity was achieved, which can be attributed to the dynamic assembly of DNA hairpins in a bidirectional manner.

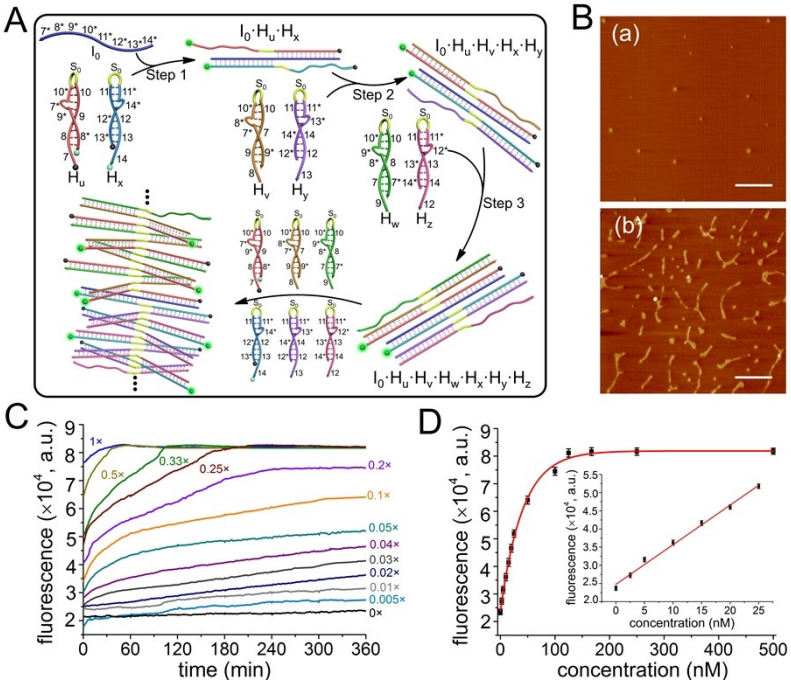

Fig. S7 (A) Schematic diagram of DHA in a bilateral growth manner. (B) AFM images of the hairpin assembled products obtained without I_0 (a) and with 0.5× I_0 (b). Scale bar: 1 μm. The concentration of each hairpin initially added is 2 μM (1×). The reactions are performed at 25 °C for 6 h. (C) Fluorescence kinetics of the DHA initiated by different concentrations of I_0 in a bilateral growth manner. The concentration of each hairpin initially added is 10 μM (1×). (D) The calibration curve plotted with the fluorescence intensity at 6 h against the final concentration of I_0. Inset: linear fit of the plot when the final concentration of I_0 is from 2.5 to 25 nM. Note: the initial 0.01× corresponds

to a final concentration of 5 nM. The relative fluorescence intensity is calculated by $F-F_0$, where F_0 and F are the fluorescence intensities without and with target DNA, respectively. Error bars indicate the standard deviations of three independent measurements.